Self-bearing Motor with DSP Based Control System*

Rafael R. Gomes and Richard M. Stephan
LASUP –Laboratory of Applied Superconductivity
Universidade Federal do Rio de Janeiro
Cidade Universitária, Rio de Janeiro, Brazil
ramos@ufrj.br,rms@ufrj.br

José A. Santisteban
Escola de Engenharia/TEE/PGMEC
Universidade Federal Fluminense (UFF)
Rua Passo da Pátria, 156 - Niterói - RJ - Brazil
jasl@mec.uff.br

***Abstract* – This paper presents an adaptive digital controller for a self-bearing motor. The controller is implemented using a DSP platform. Initially, the motor operation is explained and a mathematical model derived. The optimized performance is achieved adjusting the controller parameters as a function or the rotor angular speed. Finally, some characteristics of the DSP implementation are described.**

***Key words* – Bearingless machines, Magnetic bearings, High-speed electric motors, Feedback control systems, Emerging technologies.**

I. Introduction

The advantages of self-bearing motors, also called bearingless motors, encourage research groups all over the world to design their own prototypes [1][2][3][4]. This technology allows the construction of frictionless motors, eliminating the need of lubrication and expanding the velocity operation limits. These characteristics open a wide range of applications in industrial, medical and aerospace fields.

Digital Signals Processors (DSP's) are powerful tools in the control of self-bearing motors [5][6]. The DSP allows real-time control, making on-line controller parameters adjustments in function of the rotor velocity possible.

This work presents a DSP implementation of a self-bearing motor control. The model, the implementation and the operation are explained.

II. Self Bearing Motor

The self-bearing motor is a device that combines both the rotor radial positioning and the torque production. To make this operation possible, a feedback control system is necessary. This feedback control monitors the rotor position constantly and produces electromagnetic forces to restore the shaft position. These electromagnetic forces can be produced with differential currents imposed on each stator pole.

The prototype considered here consists of a pair of four poles, two phases induction motors. Figure 1 shows a cute-view of this self-bearing motor.

The rotors of these motors were assembled together on one vertical axis. The axis can be supported by a superconductor axial bearing [7][8].

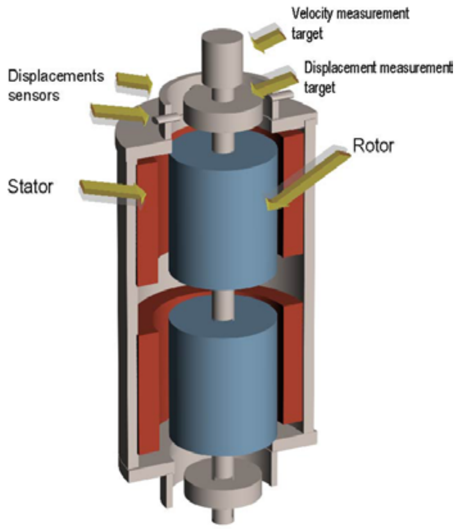

Figure 1: Self-bearing motor cute-view.

The system admits a maximum radial gap of 0.4*mm* between the security bearing and the stator.

The displacement is measured by eddy current sensors [9]. Figure 2 shows the disposition of these sensors. A cylindrical conductor target is placed in the center and connected to the motor shaft

A set of two oposite sensors (x-x' or y-y') provides voltage levels with linear variations of the radial displacement

Connected to the displacement target there is another cylinder with longitudinal gaps to determine the rotor velocity using a fifth inductive sensor.

III. Electromechanical Model

A two phase, four poles induction model was used. In phase A, each pole winding can be independently controlled. In phase B, all windings are series connected. The positioning currents are imposed to phase A windings in a differential way. In equilibrium state, the rotor shaft is centralized and all currents applied to the four A phase windings have the same value. In this case, no radial force is produced. Figure 3 shows the stator windings.

If the rotor is decentralized, a non-zero value of differential current is used to produce the restoration forces to move the rotor to the central position. This is accomplished by reducing the current amplitude applied to one pole winding and increasing the current amplitude of the other pole winding on the same direction. Figure 4 shows the control system implementation model.

* This work is partially supported by CNPq and CAPES Grants.

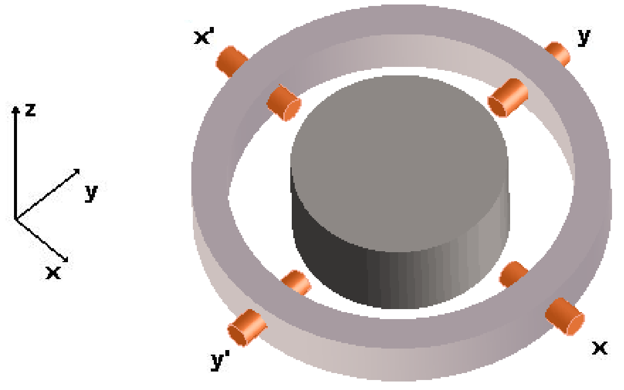

Figure 2: Displacement sensors disposition.

In this manner, the currents have the following expressions:

$$i_{y1} = (i_0 + \Delta i_y)\cos\omega t\,, \tag{1}$$
$$i_{y2} = (i_0 - \Delta i_y)\cos\omega t\,, \tag{2}$$
$$i_{x1} = (i_0 + \Delta i_x)\cos\omega t\,, \tag{3}$$
$$i_{x2} = (i_0 - \Delta i_x)\cos\omega t\,. \tag{4}$$

The radial forces are related to the differential currents by:

$$F_{y1} = -\frac{1}{4}N^2\mu\frac{A}{y^2}\left[8 i_0 \Delta i_y\right]\cos^2\omega t\,, \tag{5}$$

$$F_{y2} = -\frac{1}{4}N^2\mu\frac{A}{y^2}\left[-8 i_0 \Delta i_y\right]\cos^2\omega t\,, \tag{6}$$

$$F_y = F_{y1} - F_{y2}\,. \tag{7}$$

The force F_y can be considered directly proportional to Δi_y for small displacements (y approximately constant).

Similar equations con be obtained for the orthogonal direction x.

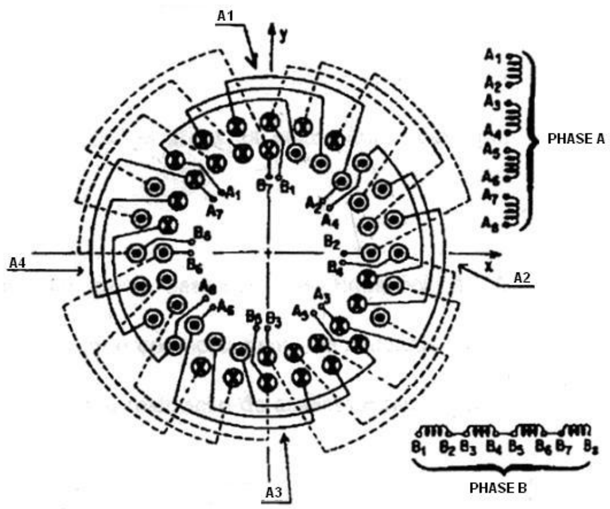

Figure 3: Stator windings

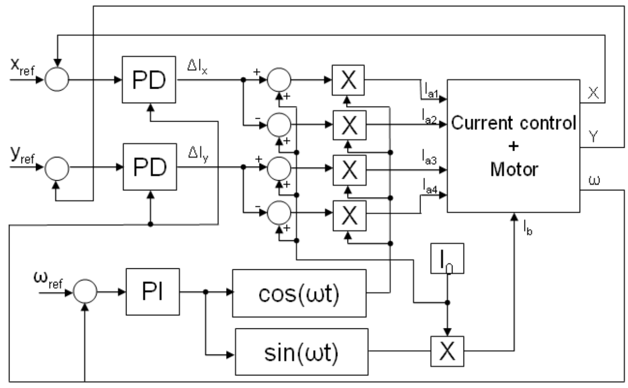

Figure 4. Control system implementation model.

The term $\cos^2 \omega t$ can also be decomposed in:

$$\cos^2\omega t = \frac{1}{2}\left(1 + \cos 2\omega t\right), \tag{8}$$

showing two components:

- a continuous force and
- an harmonic force.

As long as the natural frequencies of the rotor are kept reasonably lower than the harmonic frequency, the oscillatory term will produce a negligible effect on the dynamic behaviour of the system.

According to the schematic drawing of a vertical rotor pivoted on a point "O", shown in figure 5, and assuming, small displacements, the rotational angles α and β are given by:
$\alpha = -y/d$
$\beta = x/d$.
The following equation can be written:

$$\begin{bmatrix} I_0 & 0 \\ 0 & I_0 \end{bmatrix}\begin{Bmatrix} \ddot{y} \\ \ddot{x} \end{Bmatrix} + \begin{bmatrix} 0 & -I_p\Omega \\ I_p\Omega & 0 \end{bmatrix}\begin{Bmatrix} \dot{y} \\ \dot{x} \end{Bmatrix} = \begin{Bmatrix} bdF_y \\ bdF_x \end{Bmatrix}. \tag{9}$$

Where:
I_0 is the transversal moment of inertia at point "O";
I_p is the moment of inertia of the rotor;
Ω its spin velocity.

This matrix equation can be presented as system of two differential equations:

$$\ddot{x} = \frac{I_p}{I_0}\Omega\dot{y} + \frac{bd}{I_0}F_x\,, \tag{10}$$

$$\ddot{y} = -\frac{I_p}{I_0}\Omega\dot{x} + \frac{bd}{I_0}F_y\,. \tag{11}$$

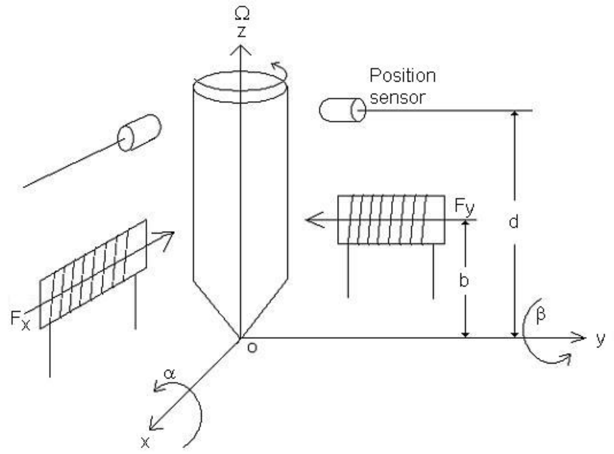

Figure 5. Electromechanical model.

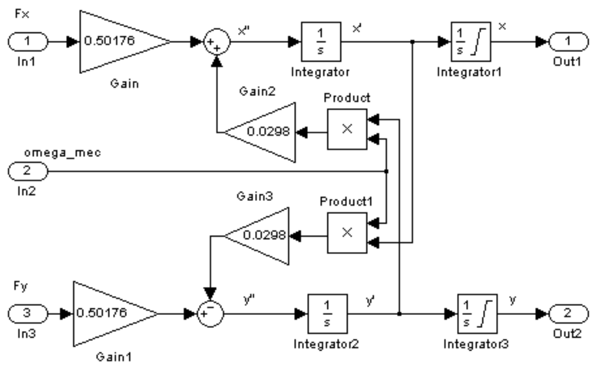

Figure 6. Block diagram of the mechanical model.

IV. Simulation Model

The simple mechanical model given by (10) and (11) allows, in a first approximation, the study of the system behavior with different types of controllers and parameters. Figure 6 shows the simulation model. The moments of inertia I_0 and I_p of the prototype were measured and found to be:

I_0= 0.134078 kg-m^2,
Ip= 0.003996 kg-m^2,
while the heights "*b*" and "*d*" are:
b= 0.195 m,
d= 0.345 m.

A simple PD controller may be used to stabilize the rotor position for each control axis [10]. However, if the rotor velocity is not taken into account to adjust the PD controller parameters, the dynamic behaviour will strongly vary, principally at high velocities of operation. This effect is known as gyroscopic effect. Figure 7 shows the system behaviour for three velocities assuming the employment of fixed and variable PD controller parameters. It can be seen that the gyroscopic effect at high velocities is larger than at lower velocities. The PD parameters should be adjusted to make an optimized performance in function of rotor velocity to minimize the gyroscopic effect.

V. Optimized Controller Design

Based on the mathematical model developed in section IV, an optimized controller, with consideration of rotor velocity, can be constructed [11]. This optimized controller parameter can be accomplished simulating the system behaviour. The best result, *i.e.*, the result with smaller overshoot, is selected as the optimized parameter for each considered rotor velocity. The diagram model of this control system is shown in Fig. 8. Figure 9 shows these optimized parameters in function of rotor velocity.
Employing a quadratic interpolation, a function for the derivative parameter can be determined. The expression of derivative parameter in function of rotor velocity is given by (12). The complete transfer function of compensator is given by (13).

$$D = -0.006\omega^2 + 0.5316\omega + 58.12 \tag{12}$$

$$C(s) = P + \frac{Ds}{(1/N)s + 1} \tag{13}$$

where N is a value of pole to make the PD controller properly. Usually this value is 10.

Figure 7(a) shows the behaviour for slow velocities. The difference is more sensible at high velocities shown in Figs.7 (b) and (c). This type of control is known as programmable adaptive control or scheduled adaptive control and may be implemented by means of lookup tables.

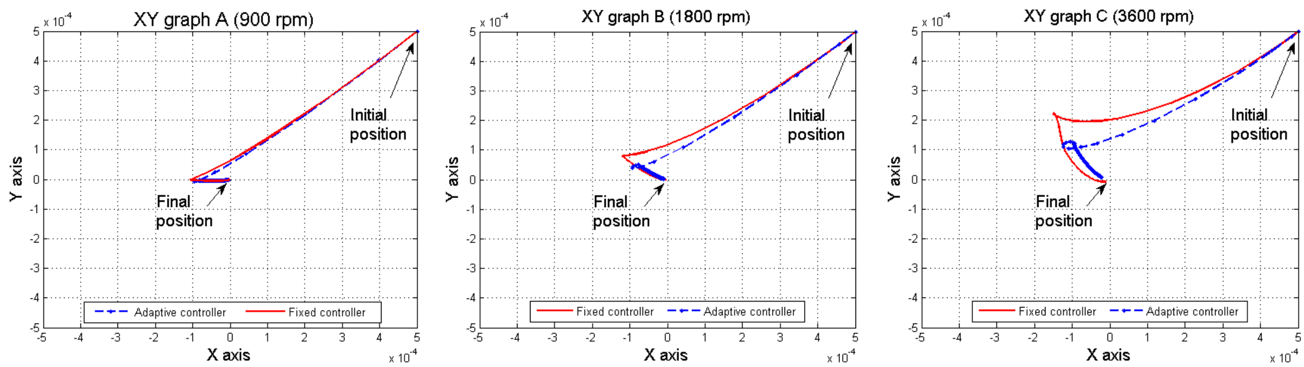

Figure 7. Simulated transient responses for fixed and adaptive PD parameters (initial condition x=0.5mm, y=0.5mm).
a) 900 rpm, b) 1800 rpm, c) 3600 rpm.

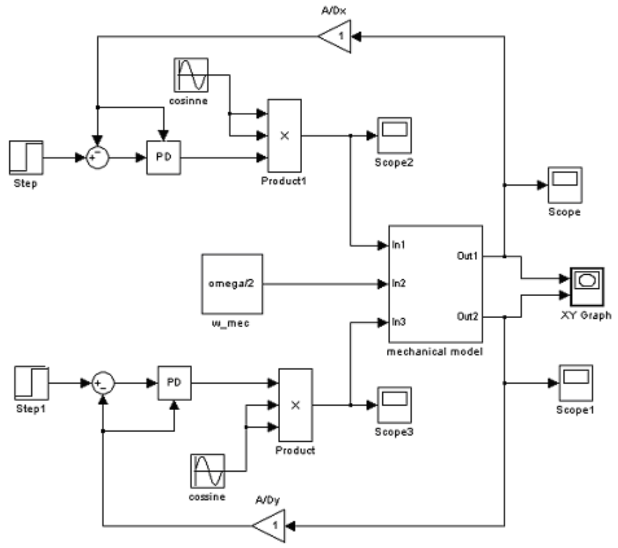

Figure 8. Diagram model of the control system.

VI. Control System Implementation Model

Based on this electromechanical model, a parameter scheduled controller was designed. The control software was developed in F2812 Texas Instruments digital signal processor. This fixed point processor requires an algorithm which uses fixed point arithmetic. The program was written in C.

The currents signals are acquired by Hall Effect current sensors. These signals are conditioned to ADC voltage levels. The digital outputs are used for produce trigger signals to an IGBT bridge.

The DSP controller has the following characteristics:

- Sampling rate: 32.779 kHz
- Numbers of AD converters: 7
- AD converters resolution: 12 bits
- Size of the control algorithm: 167kb

The sampling rate is given by frequency value which completes one 16 bits buffer (65536 different values) in two seconds. This allows the DSP generate sinusoidal frequencies in 0.5 Hz steps. The software algorithm makes the current control comparing the real current value acquired by currents sensors with the reference value generated internally on DSP. This current control uses five channels of 12 bits ADC, four to each phase A winding and one to phase B. Another two ADC channels are used for displacement sensors.

The current control was implemented in the same algorithm. The signals cos(ωt) and sin(ωt) are internally created using look-up tables.

An independent PI controller was used for the velocity control loop.

VII. Conclusions

This work presented the operation and control of a self-bearing motor using a DSP. The DSP offers a reliable and flexible implementation platform. Optimized controllers were implemented to improve the dynamic behavior of the system.

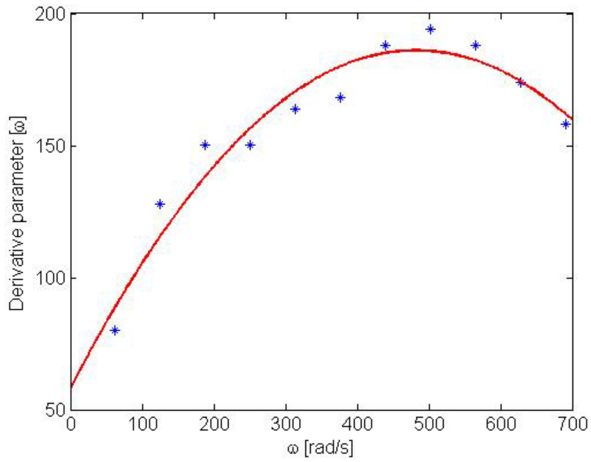

Figure 9. Optimized parameters in function of rotor velocity.

References

[1] J. A. Santisteban, "*Estudo da influência da carga torcional sobre o posicionamento radial de um motor-mancal*", D.Sc. Thesis, COPPE/UFRJ, Rio de Janeiro, Brazil, March, 1999.

[2] J. A. Santisteban, R.M Stephan. "Modelling and Analysis of a Loaded Bearingless Machine". *EPE Journal*, 2000, pp.35-39.

[3] SCHWEITZER, Gerard; BLEULER, Hannes; TRAXLER, Alfons, "Active magnetic bearings". *vdf Hochschul-verlag AG na der ETH Zurich*, Suíça, 1994,240p.

[4] A. Chiba, T. Fukao, O. Ichikawa, M. Oshima, M. Takemoto, D. Dorrell, "*Magnetic Bearings and Bearingless Drives*", Elsevier.

[5] H. Bleuler, C. Gähler, R. Herzog, R. Larsonneur, "Application of Digital Signal Processor for Industrial Magnetic Bearing*", IEEE Transactions on Control Systems Technology*, Vol. 2, No 4, December, 1994.

[6] C. R. Knospe, S. J. Fedigam, R. W. Hope, R. D. Williams, "A Multitasking DSP Implementation of Active Magnetic Bearing Control", IEEE Transaction on Control Systems Technology, Vol. 5, No 2, March, 1997.

[7] Santisteban, J.A.; David, D.F.B.; Stephan, R.M.; Ripper, A.; de Andrade, R., Jr.; Pereira, A.S.; Nicolsky, R.; "Hybrid bearing for induction machine with controlled electromagnetic positioning and superconducting levitation". *Magnetics, IEEE Transactions on* Volume 36, Issue 5, Part 1, Sept 2000 Page(s):3693 – 3695.

[8] David, D., Santisteban, J., Andrade, R., Stephan, R., Ripper, A. and Nicolsky, R. "Magnetic Bearing for Induction Machine Using Active Radial Electromagnetic and Passive Axial Superconducting Components", *Intermag 99*.

[9] User's manual, model 1195-510, Shinkawa Electric Co, Tokyo, Japan.

[10] J. A. Santisteban, R.M Stephan, "Analysis and Control of a Loaded Bearingless Machine", *IEEE International Magnetic Conference*, Kyongju, Korea, May, 1999, pp.146-148.

[11] R. R. Gomes, J. A. Santisteban, R. M. Stephan, "Optimized Performance of a Motor-Bearing", *18th International Congress of Mechanical Engineering*, Ouro Preto, MG, November, 2005.